Instability of the roll/streak structure induced by free-stream turbulence in pre-transitional Couette flow

Brian F. Farrell
School of Engineering and Applied Science, Harvard University

Petros J. Ioannou* and Marios-Andreas Nikolaidis
Department of Physics, National and Kapodistrian University of Athens

(Dated: July 19, 2016)

Although the roll/streak structure is ubiquitous in both observations and simulations of pre-transitional wall-bounded shear flow, this structure is linearly stable if the idealization of laminar flow is made. Lacking an instability, the large transient growth of the roll/streak structure has been invoked to explain its appearance as resulting from chance occurrence in the free-stream turbulence (FST) of perturbations configured to optimally excite it. However, there is an alternative interpretation for the role of free-stream turbulence in the genesis of the roll/streak structure which is that FST interacts with the roll/streak structure to destabilize it. Statistical state dynamics (SSD) provides analysis methods for studying instabilities of this type which arise from interaction between the coherent and incoherent components of turbulence. Stochastic structural stability theory (S3T), which implements SSD in the form of a closure at second order, is used in this work to analyze the SSD modes arising from interaction between the coherent streamwise invariant component and the incoherent FST component of turbulence. In pre-transitional Couette flow a manifold of stable modes with roll/streak form is found to exist in the presence of small amplitude FST. The least stable mode of this manifold is destabilized at a critical value of a parameter controlling FST intensity and a finite amplitude roll/streak structure arises from this instability through a bifurcation in this parameter. Although this bifurcation has analytical expression only in SSD, it is closely reflected in both the dynamically similar quasi-linear system, referred to as the restricted non-linear (RNL) system, and in DNS. This correspondence is verified using ensemble implementations of the RNL and DNS systems. S3T also predicts a second bifurcation at a higher value of the turbulent excitation parameter that results in destabilization of the finite amplitude roll/streak equilibria. This second bifurcation is shown to lead first to time dependence of the roll/streak in the S3T system and then to chaotic fluctuation corresponding to minimal channel turbulence. This transition scenario is also verified in simulations of the RNL and DNS systems. Bifurcation from a finite amplitude roll/streak equilibrium provides a direct route to the turbulent state through the S3T roll/streak instability.

INTRODUCTION

Streamwise roll vortices and associated streamwise streaks were identified in experiments on transition in boundary layers [1] and observed in the near wall region of turbulent flows [2–4]. These observations were subsequently corroborated by direct numerical simulations (DNS) (cf. Kim *et al.* [5]) and the roll/streak structure is now understood to be central to the dynamics of turbulence in wall-bounded shear flows.

There are two distinct dynamical problems central to understanding wall-turbulence: transition from the laminar to the turbulent state and maintenance of the turbulent state. The roll/streak structure, despite being hydrodynamically stable, is commonly agreed to be involved in instigating transition from the laminar to the turbulent state in these flows. After transition this structure persists but becomes highly variable in both space and time. This time-dependent streamwise roll and streak structure is believed to be involved in the process maintaining turbulence in shear flow that is referred to as the self-sustaining process [6–9]. Moreover, this self-sustaining mechanism appears to be quite general in that it operates not only in the near-wall region but also, and independently, in the logarithmic layer [10, 11].

Our primary interest in this work is in the robust observation of the roll/streak structure in wall-bounded shear flow prior to transition and in understanding the role of this structure in the transition process. The prominence of the roll/streak in these flows presents a problem because this structure is linearly stable. The robust observation of the roll/streak structure was first rationalized by appeal to the lift-up mechanism which describes the kinematic conversion of wall normal velocity into streamwise streak velocity in sheared flows [12, 13]. This insight was later advanced by recognition that the lift-up mechanism could be subsumed into the analytical structure of generalized stability theory (GST) by which modal stability theory and non-normal transient growth analysis are united [14–16]. While modal stability analysis provides no reason to expect appearance of roll/streak structures, GST analysis predicts optimally growing perturbations with the observed form [17, 18].

The success of optimal growth theory in predicting the observed roll/streak structure in laminar wall-bounded shear flow appeared at first to be persuasive that the explanation for observations of this structure in pre-transitional flow was secure. Moreover, in the case of

laminar flow there is no known alternative mechanism. Nevertheless, there remained a lingering doubt. For one thing, there is the regularity of the spacing and amplitude of the roll/streak in experiments [19, 20], which, as remarked by Townsend [21], is characteristic of modal growth. And then there is the observation that streamwise rolls decay in amplitude if FST levels are sufficiently low, consistent with predictions based on transiently growing optimals [22–24], while rolls grow downstream in the presence of moderate levels of FST [25] which is incompatible with transient growth and suggestive of an underlying unstable mode.

While the absence of roll/streak instability in laminar wall-bounded shear flow is established, pseudospectral theory [26, 27] reveals that a highly non-normal operator, such as that of Navier-Stokes (NS) dynamics linearized about a strongly sheared flow, can be destabilized by small perturbations to the dynamical operator itself. Consistently, it was recently shown that an emergent instability of the roll/streak structure exists in the presence of operator perturbation arising from interaction between the roll/streak structure and FST [28]. This nonlinear instability does not have analytical expression in the linearized NS dynamics of the laminar flow because the perturbations to the dynamical operator that destabilize it do not arise from a linear instability of the laminar shear flow dynamics but instead arise from systematic organization by the roll/streak structure of the Reynolds stress associated with the incoherent background of FST. The analytical expression for this instability is contained in the equations for the associated statistical state dynamics (SSD). The formulation of SSD used in this work, referred to as S3T, is a second order closure in which full nonlinearity is retained in the streamwise mean equation while the dynamics of the perturbation covariance is linearized about the instantaneous streamwise mean flow. Nonlinear interaction occurs between the mean flow dynamics (defined as flow components with streamwise wavenumber $k_x = 0$) and the perturbation covariance obtained from flow components with streamwise wavenumber $k_x \neq 0$. This quasi-linear formulation is referred to as the restricted nonlinear (RNL) approximation to the nonlinear Navier–Stokes dynamics (NL). Because the nonlinear perturbation-perturbation interactions have been neglected in the perturbation equation, RNL/S3T does not support a classical turbulent cascade. Consistent with our interpretation of RNL as an approximation to the S3T version of SSD, the perturbation equation in RNL is used only to calculate an approximate covariance. One consequence of this is that phase information is not retained for the perturbation fields, only their second order correlations being relevant to this second order SSD.

The approximation to the perturbation covariance obtained using RNL dynamics can be improved by forming a mean covariance from the covariances obtained from an ensemble of RNL perturbation equations sharing a single mean flow. In the case that an N-member ensemble is used to approximate the covariance the SSD approximation is referred to as RNL_N (cf. Constantinou *et al.* [11], Thomas *et al.* [29]). In the limit $N \to \infty$ S3T dynamics is recovered. RNL has the advantage that it can be easily implemented at high resolution while retaining the analytical restrictions of S3T. Moreover, simulations made using RNL can be compared to the same DNS implementation that was restricted to obtain the RNL system.

Further insight can be obtained by proceeding similarly with the NS equations, formally writing the full dynamics in mean/perturbation form and then calculating an ensemble average second order closure using an N-member ensemble of perturbation equations sharing a single mean flow in a manner parallel to the method used in constructing RNL_N but retaining full nonlinearity in the individual perturbation equations of the ensemble. This closure will be referred to as NL_N. When it converges NL_N corresponds to a complete cumulant expansion of the SSD solved up to second order. We find that in our example problem satisfactory convergence of RNL_N and NL_N is obtained for N as small as 10.

Consider a Couette flow subjected to a random excitation that is statistically streamwise and spanwise homogeneous and has zero mean with respect to time and space averaging. S3T predicts a bifurcation occurring at a critical amplitude of the FST excitation in which an unstable roll/streak structure emerges as an instability of the S3T dynamics. As the FST excitation is increased at first the streamwise and spanwise averaged mean flow differs little from the laminar Couette profile while superimposed on this profile is a fixed point finite amplitude roll/streak structure. With further increase in the excitation amplitude another critical value is exceeded at which the flow transitions to turbulence. The existence of these three statistical regimes under increasing FST excitation: the near laminar state, the near laminar with superimposed finite amplitude equilibrated roll/streak structure, and the turbulent regime characterized by chaotic fluctuation of the roll/streak structure in Couette flow was predicted using S3T [28]. The purpose of this paper is to determine whether these predictions made using S3T are reflected in RNL and NL and to analyze the convergence to the S3T predictions obtained using the RNL_N and NL_N approximations as $N \to \infty$.

FORMULATION OF S3T

Consider a plane Couette flow with streamwise direction x, wall-normal direction y and spanwise direction z in which FST is maintained by stochastic excitation applied throughout the flow. The lengths of the channel in the streamwise, wall-normal and spanwise direction are respectively L_x, $2h$ and L_z. The chan-

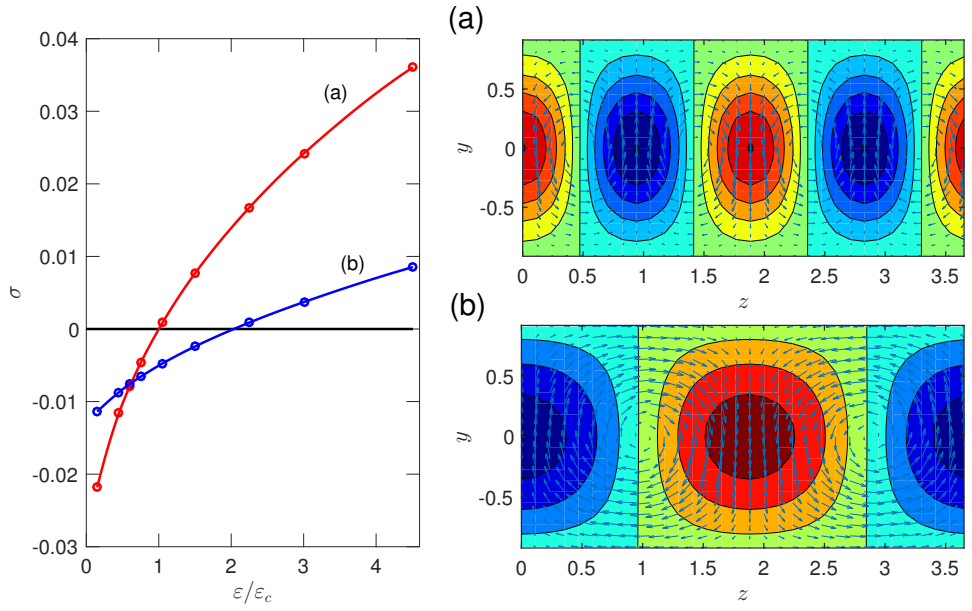

FIG. 1: Left: Growth rate of the two most unstable S3T eigenfunctions about the spanwise homogeneous S3T equilibrium as a function of the FST excitation parameter ε. Right: The structure of the corresponding eigenfunctions with growth rate (a) and (b) at FST excitation parameter $\varepsilon/\varepsilon_c = 2$. Shown are contours of the streak velocity, U_s, and velocity vectors of the components (V, W) plotted on a (y, z) plane cross-section. The structure of these eigenfunctions does not change appreciably for $\varepsilon/\varepsilon_c < 6$. At $\varepsilon = \varepsilon_c$ the S3T spanwise uniform equilibrium bifurcates to a finite amplitude equilibrium with perturbation structure close to that of the most unstable eigenfunction shown in (a). The channel is minimal with $L_x = 1.75\pi$ and $L_z = 1.2\pi$, the Reynolds number is $R = 400$, and the stochastic forcing excites only Fourier components with streamwise wavenumber $k_x = 2\pi/L_z = 1.143$. Stochastic excitation of the Couette flow at amplitude ε_c would sustain perturbation energy 0.14% of Couette flow energy.

nel walls are at $y/h = -1$ and 1. Spatial and temporal averages are denoted by square brackets with a subscript denoting the independent variable over which the average is taken, i.e. spanwise averages by $[\cdot]_z = L_z^{-1}\int_0^{L_z}\cdot\,\mathrm{d}z$, time averages by $[\cdot]_t = T^{-1}\int_0^{T}\cdot\,\mathrm{d}t$, with T sufficiently long. Multiple subscripts denote an average over the subscripted variables in the order they appear, i.e. $[\cdot]_{x,y} \stackrel{\text{def}}{=} [[\cdot]_x]_y$. The vector velocity $\mathbf{u}$ is decomposed into its streamwise mean, denoted by $\mathbf{U}(y,z,t) \stackrel{\text{def}}{=} [\mathbf{u}(x,y,z,t)]_x$, and the deviation from this mean (the perturbation) denoted $\mathbf{u}'(x,y,z,t)$ so that $\mathbf{u} = \mathbf{U} + \mathbf{u}'$. The pressure gradient is similarly decomposed as $\nabla p = \nabla\left(P(y,z,t) + p'(x,y,z,t)\right)$. Velocity is non-dimensionalized by the velocity at the wall, U_w, at $y/h = 1$, lengths by h, and time by h/U_w. The non-dimensional NS equations decomposed into an equation for the mean and an equation for the perturbation are:

$$\partial_t \mathbf{U} + \mathbf{U}\cdot\nabla\mathbf{U} + \nabla P - \Delta\mathbf{U}/R = -\left[\mathbf{u}'\cdot\nabla\mathbf{u}'\right]_x \ , \tag{1a}$$

$$\partial_t \mathbf{u}' + \mathbf{U}\cdot\nabla\mathbf{u}' + \mathbf{u}'\cdot\nabla\mathbf{U} + \nabla\mathbf{p}' - \Delta\mathbf{u}'/R = \\ = -\left(\mathbf{u}'\cdot\nabla\mathbf{u}' - \left[\mathbf{u}'\cdot\nabla\mathbf{u}'\right]_x\right) + \sqrt{\varepsilon}\ \mathbf{f}'(x,y,z,t) \ , \tag{1b}$$

$$\nabla\cdot\mathbf{U} = 0 \ , \quad \nabla\cdot\mathbf{u}' = 0 \ , \quad \nabla\cdot\mathbf{f}' = 0 \tag{1c}$$

where $R = U_w h/\nu$ is the Reynolds number. The velocities and the stochastic excitation $\mathbf{f}'$ satisfy periodic boundary conditions in the z and x directions and no-slip boundary conditions in the cross-stream direction: $\mathbf{U}(x,\pm1,z,t) = (\pm1,0,0)$, $\mathbf{u}'(x,\pm1,z,t) = \mathbf{f}'(x,\pm1,z,t) = 0$. The stochastic excitation is applied only to the streamwise varying Fourier components of the flow. It is nondivergent, has zero ensemble mean, $\langle\mathbf{f}'\rangle = 0$ (the ensemble mean over excitation realizations being denoted $\langle\cdot\rangle$) , and is delta correlated in time and statistically homogeneous in the x and z directions. Delta correlation in time of the excitations implies that the energy input by the stochastic excitation is independent of the flow state and can be parameterized by ε in (1b).

The x, y, z components of $\mathbf{U}$ are (U, V, W) and the corresponding components of $\mathbf{u}'$ are (u', v', w'). The streak component of the streamwise mean flow is denoted by U_s and defined as

$$U_s \stackrel{\text{def}}{=} U - [U]_z \ . \tag{2}$$

The streamwise mean cross-stream and spanwise velocities, V and W, are found to primarily constitute the roll vortices. We also define the streak energy density, $E_s = \left[U_s^2/2\right]_{y,z}$, the roll energy density, $E_r = \left[(V^2+W^2)/2\right]_{y,z}$, and the perturbation energy density $E_p = \left[|\mathbf{u}'|^2/2\right]_{x,y,z}$. Energy is injected from the moving walls at rate $I = (2R)^{-1}\left[\partial_y U|_{y=1} + \partial_y U|_{y=-1}\right]_z$ and at rate ε from the appropriately normalized stochastic forcing. Energy is dissipated at rate $D = R^{-1}\left[|\nabla\times\mathbf{u}|^2\right]_{x,y,z}$. With I_c and D_c we denote the energy injection and dissipation rates of the Couette flow.

The S3T dynamics is a SSD governing the evolution of the first two cumulants consisting of the streamwise mean flow, $\mathbf{U} = (U, V, W)$ or $\mathbf{U} \stackrel{\text{def}}{=} (U_x, U_y, U_z)$, and the second cumulants that are the same time covariances of the Fourier components of the velocity fluctuations, $\hat{u}'_{\alpha,k_x}$, where the index $\alpha = x, y, z$ indicates the velocity component in the Fourier expansion of the perturbation velocity $\mathbf{u}'$:

$$\mathbf{u}'(x,y,z,t) = \sum_{k_x>0} \mathrm{Re}\left(\hat{\mathbf{u}}'_{k_x}(y,z,t)\, e^{ik_x x}\right) \ , \tag{3}$$

with k_x the streamwise wavenumbers that are excited by the stochastic excitation. We similarly expand the excitation in its Fourier components $\hat{\mathbf{f}}'_{k_x}$. In this study we will limit the stochastic excitation to only the streamwise fundamental wavenumber $k_x = 2\pi/L_x$ and as a result the subscript k_x in the velocity and excitation components can be dropped without ambiguity. Because in the S3T equations the perturbation-perturbation interactions are not included, this choice of excitation implies that the S3T flow field perturbations have power only at the streamwise component that is forced. The covariance variables of S3T are the covariances of the velocity components of Fourier component k_x between point $1 \stackrel{\text{def}}{=} (y_1, z_2)$ and point $2 \stackrel{\text{def}}{=} (y_2, z_2)$ evaluated at the same time:

$$C_{\alpha\beta}(1,2) = \left\langle \hat{u}'_\alpha(1)\hat{u}'^*_\beta(2)\right\rangle \ , \tag{4}$$

which is a function of the coordinates of the two points (1) and (2) on the (y, z) plane and of time ($*$ denotes complex conjugation). The S3T equations are:

$$\begin{aligned}\partial_t U_\alpha + U_\beta\partial_\beta U_\alpha + \partial_\alpha P - \Delta U_\alpha/R &= \\ = -\frac{1}{2}\,\mathrm{Re}\left(\partial_y C_{y\alpha}(1,1) + \partial_z C_{z\alpha}(1,1)\right) \ ,& \end{aligned} \tag{5a}$$

$$\begin{aligned}\partial_t C_{\alpha\beta}(1,2) =& A_{\alpha\gamma}(1)C_{\gamma\beta}(1,2) + A^*_{\beta\gamma}(2)C_{\alpha\gamma}(1,2) \\ &+ Q_{\alpha\beta}(1,2) \ ,\end{aligned} \tag{5b}$$

$$\partial_a U_a = 0 \quad , \quad \hat{\partial}_\alpha(1)C_{\alpha\beta}(1,2) = \hat{\partial}^*_\beta(2)C_{\alpha\beta}(1,2) = 0 \ , \tag{5c}$$

with summation convention on repeated indices and the operator $\hat{\partial} \stackrel{\text{def}}{=} (ik_x, \partial_y, \partial_z)$ (for a derivation cf. [28]). The operator $A_{\alpha\beta}(1)$ (or $A_{\alpha\beta}(2)$) is the operator governing the quasi-linear evolution of streamwise varying perturbations in (1b) with streamwise wavenumber $k_x = 2\pi/L_x$ linearized about the instantaneous streamwise mean flow $\mathbf{U}(1)$ (or $\mathbf{U}(2)$) and 1 (or 2) indicates that the operator acts on the 1 (or the 2) variable of $C(1,2)$. $Q_{\alpha\beta}(1,2)$ are the spatial covariances of the k_x Fourier components of the forcing components, $\hat{f}_i$, and are defined as

$$\left\langle \hat{f}_\alpha(1,t_1)\hat{f}^*_\beta(2,t_2)\right\rangle = \delta(t_1-t_2)Q_{\alpha\beta}(1,2) \ . \tag{6}$$

Using S3T we can find roll/streak structures that are independent of time because their forcing derives from a converged covariance obtained from an equivalently infinite ensemble of independent realizations. These fixed point equilibria are imperfectly reflected in individual realizations because fluctuations in the covariance arise due to the finiteness of the equivalent ensemble of statistically independent structures that fit in the channel. These fluctuations in the covariance result in imperfect correspondence with the underlying equilibrium structure revealed by S3T (cf. [30, 31]). In order to verify that the S3T fixed point does in fact underly the dynamics of the roll/streak structure observed in RNL and NS it is useful to obtain solutions lying on the continuum from the single realization solution to the infinite ensemble S3T fixed point solution. S3T dynamics is approached by RNL_N simulations as $N \to \infty$. The RNL_N system is governed by the system of equations

$$\partial_t \mathbf{U} + \mathbf{U}\cdot\nabla\mathbf{U} + \nabla P - \Delta\mathbf{U}/R = -\left\langle[\mathbf{u}'\cdot\nabla\mathbf{u}']_x\right\rangle_N \ , \tag{7a}$$

$$\begin{aligned}\partial_t \mathbf{u}'_n + \mathbf{U}\cdot\nabla\mathbf{u}'_n + \mathbf{u}'_n\cdot\nabla\mathbf{U} + \nabla\mathbf{p}'_n - \Delta\mathbf{u}'_n/R &= \\ = \sqrt{\varepsilon}\ \mathbf{f}_n{}'(x,y,z,t) \ ,& \end{aligned} \tag{7b}$$

$$\nabla\cdot\mathbf{U} = 0 \ , \quad \nabla\cdot\mathbf{u}'_n = 0 \ , \quad \nabla\cdot\mathbf{f}'_n = 0 \tag{7c}$$

where $n = 1, \cdots, N$ indicates the ensemble member, and $\langle\cdot\rangle_N$ indicates an average over the N ensemble members. Note that in correspondence with S3T dynamics the perturbation-perturbation interaction in (1b) is ignored.

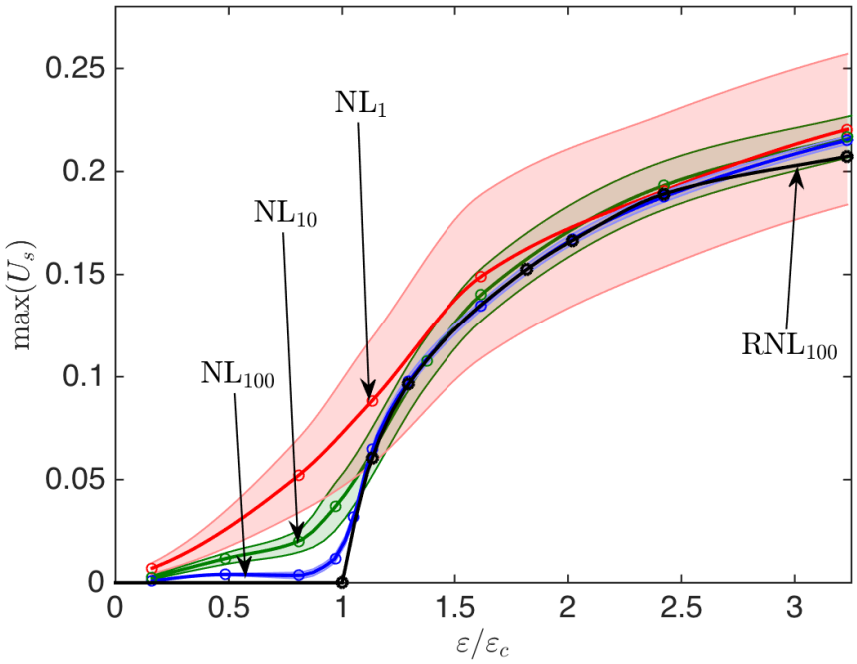

FIG. 2: Bifurcation diagram for the Couette problem. Shown is the time mean of the maximum value of the streak amplitude, U_s as a function of the stochastic excitation amplitude, ε, for an NL$_1$ simulation (red), an ensemble NL$_{10}$ simulation (green), an ensemble NL$_{100}$ simulation (blue), and an ensemble RNL$_{100}$ simulation (black). The critical bifurcation value has been determined from stability analysis of the S3T system and it has been confirmed that this value is closely approximated using RNL$_{100}$. For $\varepsilon/\varepsilon_c < 1$, S3T predicts that the streamwise streak and roll amplitude is zero. At $\varepsilon = \varepsilon_c$ the S3T spanwise uniform equilibrium bifurcates giving rise to a finite amplitude equilibrium with roll and streak. The NL$_1$ and NL$_{10}$ simulations exhibit fluctuating streak/roll structures and one standard deviation of the fluctuations correspond to the shaded regions in the figure. The fluctuations in the ensemble NL$_{100}$ and RNL$_{100}$ simulations are small and only those associated with NL$_{100}$ are shown. Other parameters as in Fig. 1.

In a similar manner we can define ensemble NL$_N$ simulations correspond to the first two components of a converged expansion in cumulants. NL$_N$ is governed by the system of equations:

$$\partial_t \mathbf{U} + \mathbf{U}\cdot\nabla\mathbf{U} + \nabla P - \Delta\mathbf{U}/R = -\left\langle [\mathbf{u}'\cdot\nabla\mathbf{u}']_x \right\rangle_N \ , \tag{8a}$$

$$\partial_t \mathbf{u}'_n + \mathbf{U}\cdot\nabla\mathbf{u}'_n + \mathbf{u}'_n\cdot\nabla\mathbf{U} + \nabla\mathbf{p}'_n - \Delta\mathbf{u}'_n/R = \\ = -\left(\mathbf{u}'_n\cdot\nabla\mathbf{u}'_n - [\mathbf{u}'_n\cdot\nabla\mathbf{u}'_n]_x\right) + \sqrt{\varepsilon}\ \mathbf{f}_n{}'(x,y,z,t) \ , \tag{8b}$$

$$\nabla\cdot\mathbf{U} = 0 \ , \quad \nabla\cdot\mathbf{u}'_n = 0 \ , \quad \nabla\cdot\mathbf{f}'_n = 0 \tag{8c}$$

We are interested in whether the analytical predictions of the S3T equations are approached in RNL$_N$ and NL$_N$ simulations as N increases. Results are presented for the minimal Couette flow channel of [7] at $R = 400$ (based on channel half-width) with streamwise length $L_x = 1.75\pi$, spanwise length $L_z = 1.2\pi$ and channel half-width $L_y = 1$. The gravest streamwise wavenumber $k_x = 2\pi/L_x$ is stochastically excited using independent compact support cross-stream velocity and cross-stream vorticity structures in (y,z). Numerical calculations employ $N_y = 21$ grid points in the cross-stream direction and 32 harmonics in the spanwise and streamwise directions. Other stochastic excitations produce only qualitative differences in the results. A study of the S3T dynamics of this channel model was reported in [28].

COMPARISON OF ROLL/STREAK BIFURCATION AND STRUCTURE IN S3T, RNL$_N$ AND DNS$_N$

The S3T SSD (5) supports spanwise uniform fixed point solutions with streamwise mean flow form $\mathbf{U}_e = (U_e(y), 0, 0)$ and associated spanwise covariance $C_e(y_1, y_2, z_1 - z_2)$. Taking $\varepsilon = 0$, recovers the laminar Couette flow $U_e = y$ with $C_e = 0$. As ε increases the equilibrium streamwise mean flow, $U_e(y)$, departs from the Couette flow. Stability of these spanwise uniform

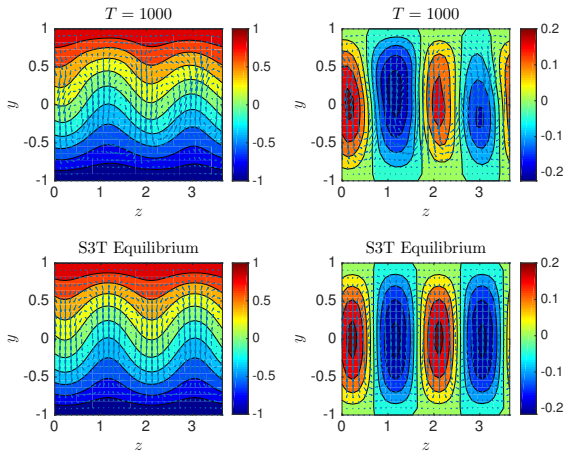

FIG. 3: Top panels: Snapshot of the streamwise mean flow from an NL_1 simulation at stochastic excitation amplitude $\varepsilon/\varepsilon_c = 3$. Shown are contours of the streamwise mean velocity U (left top), streak velocity, U_s (right top) and velocity vectors of the components (V, W) in the (y, z) plane at $t = 1000$ of the simulation. Bottom panels: The corresponding streamwise mean flow for the S3T system at $\varepsilon/\varepsilon_c = 3$. This figure shows that the equilibrium roll/streak regime predicted by S3T is reflected in single realizations of the NL equations. Parameters are as in the previous figures.

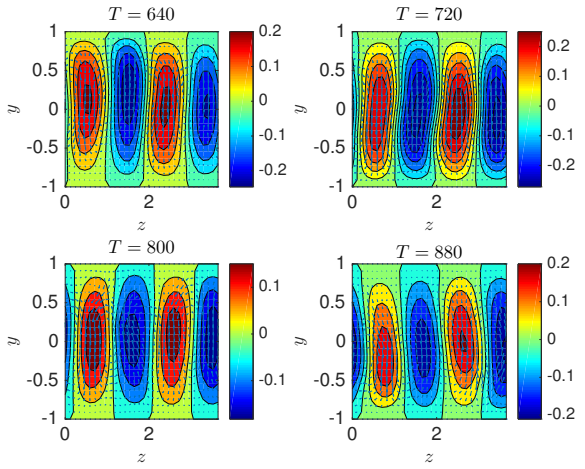

FIG. 4: Snapshots at times $t = 640,\ 720,\ 800,\ 880$ of the contours of the streak velocity, U_s, and velocity vectors of the components (V, W) plotted on a (y, z) plane cross-section from an NL_1 simulation at stochastic excitation amplitude $\varepsilon/\varepsilon_c = 3$. This figure shows the persistence of the organized structure in NL_1. This structure and its persistence stem from the underlying equilibrium state that exists for this excitation amplitude in the S3T dynamics. The other parameters are as in the previous figures.

S3T equilibria can be determined as a function of ε using the S3T equations (5) linearized about these fixed points [28].

Eigenvalues and the associated mean flow eigenfunction structure for the first two most unstable S3T modes are shown in Fig. 1. The complete associated eigenfunctions comprise both a mean flow component $(\delta U(y,z), \delta V(y,z), \delta W(y,z))$, which is shown in Fig. 1, and a covariance component $\delta C(y_1, y_2, z_1, z_2)$. The structure of the mean flow component of these eigenfunctions changes only slightly as the amplitude of the forcing, ε, increases. The eigenfunctions consist of low and high speed streamwise streaks together with roll circulations exactly collocated to reinforce the streak velocity. Despite being more highly dissipated by diffusion, the mean flow eigenfunction which becomes unstable first as ε increases is not the eigenstructure with the gravest spanwise wanumber $k_z = 2\pi/L_z = 1.67$, shown in Fig. 1b, but the second spanwise harmonic with wavenumber $k_z = 4\pi/L_z = 3.33$, shown in Fig. 1a. Destabilization of these roll/streak eigenfunctions can be traced to a universal positive feedback mechanism operating in turbulent flows: when incoherent turbulence is perturbed by a coherent streak, the streak distorts the incoherent turbulence so as to induce ensemble mean Reynolds stresses forcing streamwise mean roll circulations configured to reinforce the streak perturbation that gave rise to them (cf. [28]). The modal streak perturbations of the fastest growing eigenfunctions induce the strongest such feedback.

S3T stability analysis determines the critical excitation, ε_c, at which the spanwise homogeneous turbulent equilibrium state becomes unstable. For the parameters of our example problem this ε_c corresponds to maintaining in the Couette flow a perturbation field with mean energy density 0.14% of the energy density of the Couette flow. For $\varepsilon > \varepsilon_c$ a symmetry breaking occurs with the emergence of mean flow structures in the form of the fastest growing eigenfunction which is shown in Fig. 1a. Over a finite interval $\varepsilon_c < \varepsilon < \varepsilon_t$ the unstable S3T eigenfunction equilibrates nonlinearly to form finite amplitude S3T equilibria with roll/streak structure qualitatively similar to the corresponding eigenfunction (for our examples $\varepsilon_t/\varepsilon_c \approx 5.5$).

A bifurcation diagram showing the maximum of the streak velocity, U_s, and of the streamwise mean cross-stream velocity, V, is shown as a function of ϵ in Fig. 2 . The indicated critical ϵ_c was determined by S3T stability analysis. For $\varepsilon/\varepsilon_c < 1$ the equilibrium is spanwise independent with no coherent roll/streak structure. The equilibrium values shown in Fig. 2 were obtained using RNL_{100} simulations. These RNL_{100} equilibria have been verified to be very close to the infinite ensemble S3T equilibria.

Single NL and ensemble NL integrations allow us to study the correspondence between the infinite ensemble

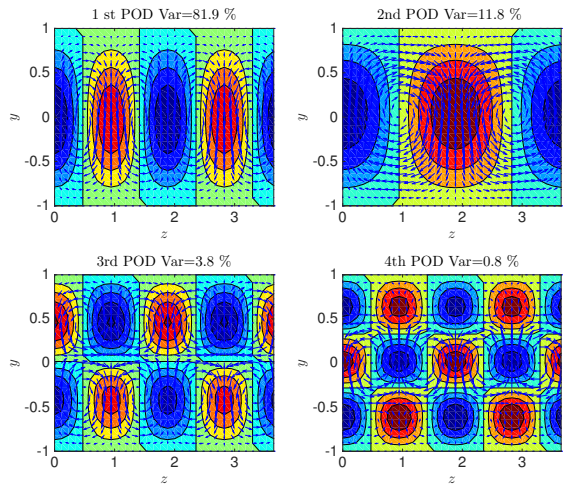

FIG. 5: Contours of streak velocity, U_s, and vectors of roll components (V, W) plotted on a (y, z) cross-section for the first 4 PODs of the streamwise mean flow fluctuations of an NL_1 forced at $\varepsilon/\varepsilon_c = 0.75$. The PODs come in pairs. The first pair of PODs which account for 82% of the energy of the fluctuations of the streamwise mean flow has the structure of the least damped S3T mode which because of the synergistic mechanism revealed by S3T is not the gravest mode in the channel. This figure shows that the fluctuations in the NL_1 simulations reveal the S3T stable modes. Other parameters as in the previous figures.

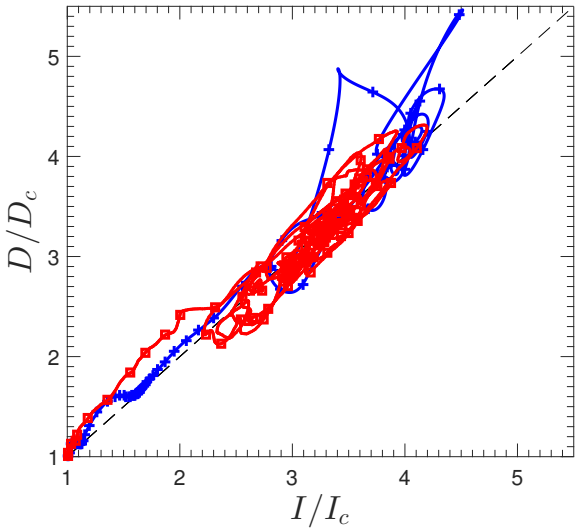

FIG. 6: Evolution of energy input rate, I/I_c and dissipation rate, D/D_c, from the laminar state to the turbulent state in an NL_1 simulation (squares-solid) and in an S3T simulation (crosses-solid) with FST excitation parameter $\varepsilon/\varepsilon_c = 9$. Symbols are marking intervals of 10 units of time. The metastable state is characterized by $D/D_c \approx 1.7$. Parameters as in the previous figures.

predictions of S3T analysis and NL turbulence. While finite ensemble simulations produce fluctuating roll/streak structures we find that even in the case of a realization simulation, corresponding to $N = 1$, a clear roll/streak structure emerges for $\varepsilon > \varepsilon_c$ which exhibits great persistence and has the same structure as that predicted by S3T analysis. An indicative comparison between an S3T equilibrium roll/streak structure and a snapshot of the corresponding roll/streak from an NL_1 simulation at $\varepsilon/\varepsilon_c = 3$ is shown in Fig. 3.

While the S3T equilibria are fixed points, the corresponding roll/streak structure in the NL_1 simulation reflect the time independence of the S3T equilibria imperfectly. However, it is persuasive that the analytical structure revealed by S3T analysis underlies the behavior seen in the NL_1 simulation; for example see the snapshots shown in Fig. 4. Noise driven fluctuations of the ensemble structure are also apparent in the bifurcation diagram shown in Fig. 2 in which the mean and variance of the maximum streak, U_s, in NL_1 and NL_{10} are indicated. The reflection of the analytical S3T bifurcation is clearly seen in the NL_{10} results and near convergence is obtained in the NL_{100} results.

We have demonstrated that the unstable roll/streak modes and associated finite amplitude S3T equilibria that are revealed by S3T analysis give rise to the structure observed in pre-transitional turbulent Couette flow in both NL and ensemble NL simulations. However, the stable S3T modes supported in the S3T stable the interval $(0 < \varepsilon/\varepsilon_c < 1)$ are also important structures in the dynamics of pre-transitional turbulence. While not excited in the fluctuation free S3T dynamics, these stable S3T modes are robustly excited by fluctuations in the forcing in NL_1 simulations (cf. [30–32]). Correspondingly, for subcritical excitation $(0 < \varepsilon/\varepsilon_c < 1)$ the mean flow of NL or ensemble NL simulations reveals a ubiquitous tendency to form roll/streak structures with temporally variable (y, z) structure arising from excitation of the stable manifold of S3T eigenmodes. A POD analysis (cf. [33]) of the streamwise mean flow reveals the dominance of this component of the variability which is accounted for by excitation of these roll/streak structures predicted by S3T (cf. [34]). For example, the first 4 POD's of NL_1 at $\varepsilon/\varepsilon_c = 0.75$, shown in Fig. 5, have the structure predicted by the S3T eigenmodes. Consistent with S3T analysis the first POD corresponds to the mode with spanwise wavenumber $k_z = 4\pi/L_z$, which corresponds to the least stable eigenfunction at this $\varepsilon/\varepsilon_c$. Note that all POD's exhibit exact alignment of the roll circulations with the streaks. This provides confirmation of the S3T prediction that these are the modal structures predicted by S3T. Consistent with these stable modes being excited by turbulent fluctuations, as $\varepsilon/\varepsilon_c \to 1$ fluctu-

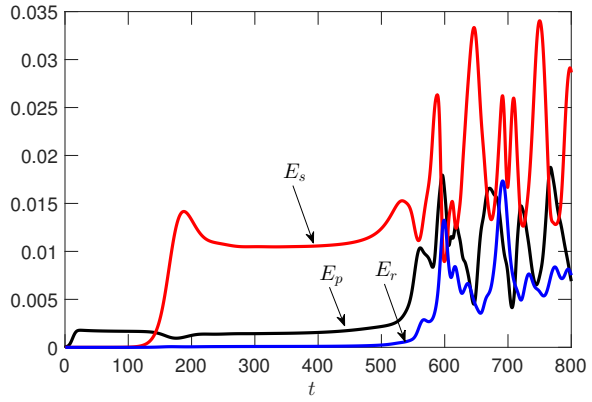

FIG. 7: Evolution of the streak energy, E_r, roll energy, E_r, and perturbation energy E_p, in an S3T integration at $\varepsilon/\varepsilon_c = 9$ under spanwise homogeneous forcing. The flow is initialized with a small random streamwise mean perturbation with spanwise dependence in order to break spanwise symmetry. The spanwise symmetric S3T equilibrium is unstable and a quasi-steady state emerges by time $t = 200$ with the roll/streak structure shown in Fig. 8. At this supercriticality the roll/streak structure (cf. Fig. 9) is an unstable fixed point of the S3T dynamics and the flow transitions to the turbulent state. Other parameters as in the previous figures.

ations of roll/streak form exhibit enhanced variance (cf. Fig. 2) which is indicative of approach to a bifurcation and is a phenomenon analogous to that of critical opalescence on approach to a fluid phase transition.

TRANSITION TO TURBULENCE

At FST excitation parameters exceeding ε_t ($\varepsilon_t/\varepsilon_c \approx 5.5$ for the chosen parameters) the finite amplitude roll/streak equilibria are no longer S3T stable and the flow transitions to a turbulent state, which is self-sustaining and persists even when the FST parameter is subsequently set to $\varepsilon = 0$ (cf. Ref. [28]). RNL_1 and NL_1 also transition to essentially similar self-sustaining turbulence. Example trajectories of transition from the laminar equilibrium state to the turbulent attractor for NL_1 and S3T are shown in Fig. 6.

A typical evolution of the perturbation energy density, E_p, streak energy density, E_s, and roll energy density, E_r, of FST excitation parameter $\varepsilon/\varepsilon_c = 9$ is shown in Fig. 7 for the case of S3T. The S3T integration was initialized with a small random streak perturbation. The flow transitions to turbulence at time $T \approx 550$. In this transition process the roll/streak emerges at first as an S3T instability which equilibrates by time $T \approx 200$ to the quasi-equilibrium finite amplitude roll/streak structure shown in the left panel of Fig. 8. This quasi-equilibrium is associated with an energy input-rate $I/I_c \approx 1.7$, which lies approximately midway between the value associated with the laminar state and that associated with the statistical mean of the turbulent state. At these parameters there exists near this quasi-equilibrium a symmetric unstable equilibrium, shown in Fig. 9, which can be converged to by suppressing spanwise asymmetries. The roll/streak structure that emerged in the S3T in the presence of realistic spanwise asymmetric perturbations breaks by exciting the unstable directions of the unstable equilibrium at about $T \approx 550$ and the flow transitions to turbulence. While this pathway to turbulence is typical in all S3T simulations with $\varepsilon > \varepsilon_t$ the timing of transition depends on the structure of the initialized state which determines the projection on the instability of the S3T equilibrium state. For example, if the flow state at $\varepsilon/\varepsilon_c = 9$ is constrained to have no perturbations breaking mirror-symmetry in the spanwise direction the flow equilibrates to the unstable roll/streak structure shown in Fig. 9 without ever transitioning to turbulence, while if the initial flow state includes a rich spectrum of such perturbations the meta-stable period is appreciably shortened.

This sequence of events, with rapid break-down of the finite amplitude roll/streak structure, is observed in NL_1 simulations at $\varepsilon/\varepsilon_c = 9$ when the simulation is initialized with the laminar state. The roll/streak structure associated with the underlying S3T instability arises at first, as in the S3T simulation, but then rapidly transitions to the turbulent state. Snapshots of the roll/streak structure during this transition, which occurs by $T = 90$, are shown in Fig. 10.

CONCLUSION

SSD makes available to analysis the manifold of nonlinear instabilities associated with the systematic organization of FST by coherent structures. In this work the S3T implementation of SSD was used to study instabilities of this type and their nonlinear extensions in a minimal channel configuration of Couette flow. At first a manifold of stable modes with roll/streak form is supported as the parameter controlling FST intensity, ε, is increased from zero. The least stable mode of this manifold is destabilized at a critical excitation designated ε_c and a finite amplitude stable fixed point with roll/streak structure arises for excitations between ε_c and a second critical value for which the finite amplitude equilibrium roll/streak is destabilized, designated ε_t. For excitation exceeding ε_t the roll/streak equilibrium is unstable to spanwise asymmetric perturbations and becomes time-dependent resulting in the establishment of the turbulent state with spanwise wavenumber approximately half that of the equilibrium state. This sequence of states

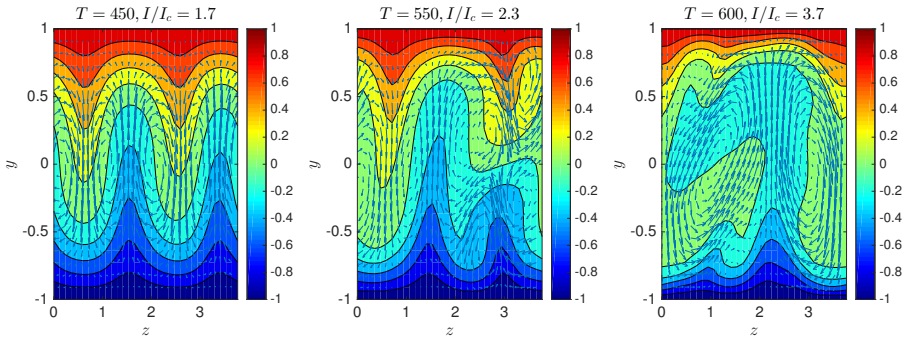

FIG. 8: Snapshots of the streamwise mean flow as it undergoes S3T transition to turbulence under stochastic forcing. Shown are contours of the streak velocity, U_s, and velocity vectors of the components (V, W) plotted on the (y, z) plane. A quasi-steady roll/streak is first formed (cf. left panel) with with input energy rate $I/I_c \approx 1.7$ and the structure of the fastest growing S3T instability (cf. Fig. 1) which has spanwise wavenumber $k_z = 4\pi/L_z$. At about $t = 550$ the flow transitions through oscillations to a turbulent roll/streak with a dominant $k_z = 2\pi/L_z$ structure. The transition period can be extended by enforcing the mirror symmetry of the streak-roll structure about the streak maximum. Other parameters as in the previous figures.

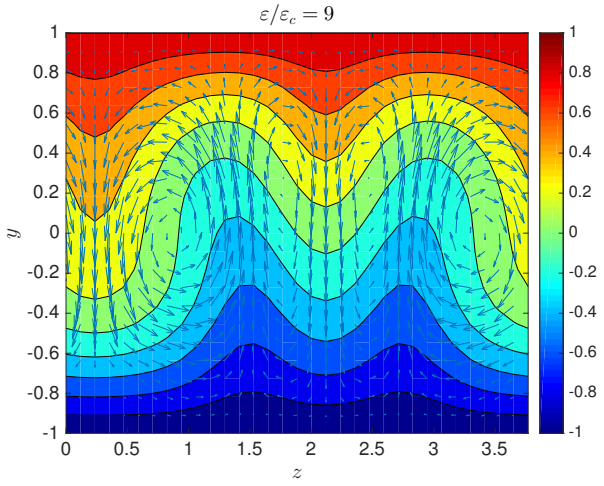

FIG. 9: The unstable roll/streak S3T equilibrium at $\varepsilon/\varepsilon_c = 9$. Shown are contours of the streak velocity, U_s, and velocity vectors of the components (V, W) plotted on a (y, z) plane cross-section. Other parameters as in the previous figures.

and transitions suggests a route to turbulence in a developing boundary layer. In order to study these SSD states and their dynamics in more detail their correspondence to realization dynamics was examined making use of a comparison among the predictions of S3T and ensemble implementations of a quasi-linear model sharing the dynamical restrictions of S3T (RNL_N) and the associated nonlinear model (NL_N). Although the SSD instabilities and their associated fixed point nonlinear equilibria and time dependent statistical mean attractor states have analytical expression only in the S3T implementation of the equivalently infinite ensemble SSD dynamics, the predicted dynamics is clearly reflected in both the dynamically similar quasi-linear system (RNL_1) and in DNS (NL_1). This correspondence was further examined using ensemble implementations of the RNL and DNS systems. As a consequence of sharing the same dynamical restrictions, the RNL_N system converges to S3T an $N \to \infty$. Remarkably, the NL_N system, which corresponds to a full closure for this problem, also converges to close correspondence with S3T as $N \to \infty$. This convergence is reflected in similar bifurcation behavior as well as similar equilibrium structures for the stable fixed point equilibria. Additionally, S3T also predicts a second bifurcation at a higher value of the turbulent excitation parameter that results in destabilization of the finite amplitude roll/streak equilibria and establishment of a turbulent state corresponding to minimal channel turbulence. This scenario constitutes a mechanism for bypass transition to the turbulent state. Comparison with NL_1 reveals that this mechanism in fact is responsible for bypass transition in the case that the transition is instigated by FST rather than by an optimal perturbation imposed at sufficiently high amplitude.

Brian Farrell was partially supported by NSF AGS-1246929. We thank Daniel Chung, Navid Constantinou, Dennice Gayme and Vaughan Thomas for helpful discussions.

* pjioannou@phys.uoa.gr

[1] P. S. Klebanoff, K. D. Tidstrom, and L. M. Sargent, J. Fluid Mech. **12**, 1 (1962).
[2] S. J. Kline, W. C. Reynolds, F. A. Schraub, and P. W. Runstadler, J. Fluid Mech. **30**, 741 (1967).

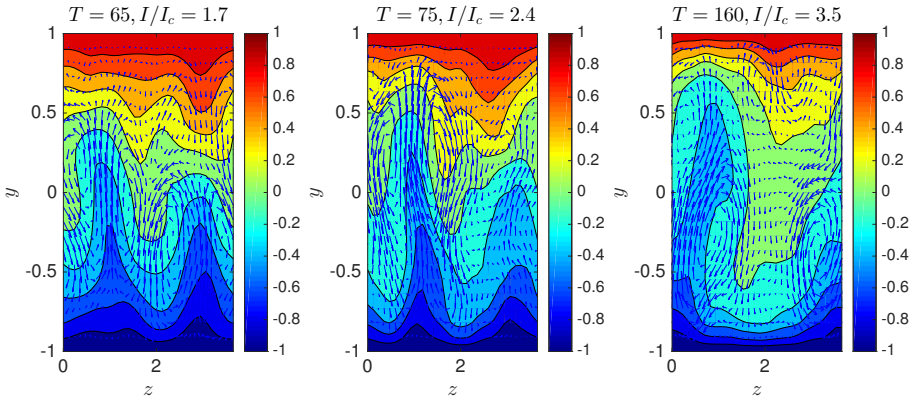

FIG. 10: Snapshots of the streamwise mean flow as it undergoes transition to turbulence in a NL_1 simulation under stochastic forcing. with $\varepsilon/\varepsilon_c = 9$. Shown are contours of the streak velocity, U_s, and velocity vectors of the components (V, W) in the (y, z) plane. A quasi-steady roll/streak initially forms, by $T = 65$, that swiftly breaks down and the flow transitions to turbulence. The transition is as in the S3T simulation (cf. Fig. 7 and Fig. 8), except that the flow passes through the metastable state rapidly. Other parameters as in the previous figures.

[3] H. P. Bakewell Jr. and L. Lumley, Phys. Fluids **10**, 1880 (1967).
[4] J. Kim, S. J. Kline, and W. C. Reynolds, J. Fluid Mech. **50**, 133 (1971).
[5] J. Kim, P. Moin, and R. Moser, J. Fluid Mech. **177**, 133 (1987).
[6] J. Jiménez and P. Moin, J. Fluid Mech. **225**, 213 (1991).
[7] K. Hamilton, J. Kim, and F. Waleffe, J. Fluid Mech. **287**, 317 (1995).
[8] W. Schoppa and F. Hussain, J. Fluid Mech. **453**, 57 (2002).
[9] J. Jiménez, Phys. Fluids **25**, 101302 (2013).
[10] Y. Hwang and C. Cossu, Phys. Fluids **23**, 061702 (2011).
[11] N. C. Constantinou, A. Lozano-Durán, M.-A. Nikolaidis, B. F. Farrell, P. J. Ioannou, and J. Jiménez, J. Phys. Conf. Ser. **506**, 012004 (2014).
[12] T. Ellingsen and E. Palm, Phys. Fluids **18**, 487 (1975).
[13] M. T. Landahl, J. Fluid Mech. **98**, 243 (1980).
[14] B. F. Farrell and P. J. Ioannou, J. Atmos. Sci. **53**, 2025 (1996).
[15] B. F. Farrell and P. J. Ioannou, J. Atmos. Sci. **53**, 2041 (1996).
[16] P. J. Schmid and D. S. Henningson, *Stability and Transition in Shear Flows* (Springer, New York, 2001).
[17] K. M. Butler and B. F. Farrell, Phys. Fluids **4**, 1637 (1992).
[18] S. C. Reddy and D. S. Henningson, J. Fluid Mech. **252**, 209 (1993).
[19] M. R. Head and I. Rechenberg, J. Fluid Mech. **14**, 1 (1962).
[20] P. Bradshaw, J. Fluid Mech. **22**, 679 (1965).
[21] A. A. Townsend, *The structure of turbulent shear flow*, 2nd ed. (Cambridge University Press, 1976).
[22] A. A. Bakchinov, M. M. Katasonov, and V. V. Kozlov, Preprint No. l-97, ITAM, Russian Academy of Sciences, Novosibirsk, Russia (in Russian) (1997).
[23] P. H. Alfredsson and M. Matsubara, in *Proc. Transitional Boundary Layers in Aeronautics*, edited by R. A. W. M. Henkes and J. L. van Ingen (Royal Netherlands Academy of Arts and Sciences. Elsevier Science Publishers, 1996) pp. 373–386.
[24] K. J. A. Westin, A. A. Bakchinov, V. V. Kozlov, and P. H. Alfredsson, Eur. J. Mech. B-Fluid **17**, 823 (1998).
[25] K. J. A. Westin, A. V. Boiko, B. G. B. Klingmann, V. V. Kozlov, and P. H. Alfredsson, J. Fluid Mech. **281**, 193 (1994).
[26] L. N. Trefethen, A. E. Trefethen, S. C. Reddy, and T. A. Driscoll, Science **261**, 578 (1993).
[27] L. N. Trefethen and M. Embree, *Spectra and Pseudospectra: The Behavior of Nonnormal Matrices and Operators* (Princeton University Press, Princeton, 2005).
[28] B. F. Farrell and P. J. Ioannou, J. Fluid Mech. **708**, 149 (2012).
[29] V. Thomas, B. K. Lieu, M. R. Jovanović, B. F. Farrell, P. J. Ioannou, and D. F. Gayme, Phys. Fluids **26**, 105112 (2014).
[30] B. F. Farrell and P. J. Ioannou, J. Atmos. Sci. **60**, 2101 (2003).
[31] B. F. Farrell and P. J. Ioannou, in *Zonal jets*, edited by B. Galperin and P. L. Read (Cambridge University Press, 2016) Chap. 5, (submitted, arXiv:1412.8290).
[32] N. C. Constantinou, B. F. Farrell, and P. J. Ioannou, J. Atmos. Sci. **71**, 1818 (2014).
[33] G. Berkooz, P. Holmes, and J. L. Lumley, Annu. Rev. Fluid Mech. **25**, 539 (1993).
[34] M.-A. Nikolaidis, B. F. Farrell, P. J. Ioannou, D. F. Gayme, A. Lozano-Durán, and J. Jiménez, J. Phys.: Conf. Ser. **708**, 012002 (2016).